Direct measurement of coherent light proportion from a practical laser source

Xi Jie Yeo,[1] Eva Ernst,[1] Alvin Leow,[2] Jaesuk Hwang,[1] Lijiong Shen,[1] Christian Kurtsiefer,[1, 2] and Peng Kian Tan[1]

[1] *Centre for Quantum Technologies, National University of Singapore, 3 Science Drive 2, Singapore 117543*
[2] *Department of Physics, National University of Singapore, 2 Science Drive 3, Singapore 117551*
(Dated: December 15, 2023)

We present a technique to estimate the proportion of coherent emission in the light emitted by a practical laser source without spectral filtering. The technique is based on measuring interferometric photon correlations between the output ports of an asymmetric Mach-Zehnder interferometer. With this, we characterize the fraction of coherent emission in the light emitted by a laser diode when transiting through the lasing threshold.

I. INTRODUCTION

The invention of lasers can be traced to work describing the emission process of the light from an atom to be spontaneous or stimulated [1]. An ensemble of atoms undergoing stimulated emission will emit coherent light that has a well-defined phase, while spontaneous emission will lead to randomly phased incoherent light [2]. **[XJ: The concept of coherent and incoherent light have also generated a fundamental interest in the statistical properties of light sources, including light sources containing a mixture of coherent and incoherent light [3–6].]** Coherent light is at the core of many applications, including interferometry [7], metrology [8], and optical communication.

In traditional models of macroscopic lasers [9–11], the emitted light is modeled to originate dominantly from stimulated emission. These models predict a phase transition of the nature of emission with increasing pump strength, separating two regimes where light emitted is either spontaneous (below threshold), or stimulated (above threshold).

However, experiments on small lasers have shown that the transition from spontaneous to stimulated emission is not abrupt [12–16]. Instead, light emitted from the laser can be described as a mixture of spontaneous and stimulated emission across a transition range.

In these experiments, the transition from spontaneous to stimulated emission was characterized by measuring the second-order photon correlation $g^{(2)}$, using a Hanbury-Brown and Twiss scheme [17]. The measurement result can be explained using Glauber's theory of optical coherence [3], where incoherent light from spontaneous emission would exhibit a "bunching" signature with $g^{(2)}(0) > 1$, while coherent light from stimulated emission exhibits a Poissonian distribution with $g^{(2)} = 1$.

The "bunching" signature associated with incoherent light has a characteristic timescale inversely proportional to its spectral width according to the Wiener-Khintchine theorem [18–20]. In a practical measurement, the amplitude of the "bunching" signature scales with the ratio of characteristic timescale of the light to the timing response of the detectors [21]. Thus, when the spectral width of incoherent light is so broad that the characteristic timescale of the "bunching" signature is smaller than the detector timing uncertainty, incoherent light may exhibit $g^{(2)} \approx 1$, like coherent light.

To overcome the limited detector timing uncertainty, a narrow band of incoherent light can be prepared with filters from a wide optical spectrum of an incoherent light source [22]. The narrow spectral width of a filtered incoherent light has a correspondingly larger characteristic coherence timescale, which may be long enough to be resolvable by the detectors.

However, for characterising the transition of a laser from spontaneous to stimulated emission, such spectral filtering presents some shortcomings. First, as spectral filtering discards light outside the transmission window of a filter, a result would be inconclusive for the full emission of the source. Second, spectral filtering requires *a priori* information or an educated guess of the central frequency and bandwidth of stimulated emission. Third, it has been shown that spectral filtering below the Schawlow-Townes linewidth of the laser results in $g^{(2)}(0) > 1$, similar to light from spontaneous emission [23].

Light emitted by a laser is also incoherent in multimode operation [24, 25], where a laser may emit coherent light in multiple transverse and/or longitudinal modes. The light in each mode may be coherent, but a combination of multiple modes may result in a randomly phased light, and therefore appear incoherent.

This motivates for methods quantifying the proportion of coherent light emitted by a source without the need for spectral filtering. A method to characterise the stimulated and spontaneous emission from a pulsed laser has been demonstrated before [26, 27].

In this paper, we present a method to quantify bounds for the proportion of coherent light for a continuous wave laser. Specifically, we investigate the brightest mode of coherent emission from a semiconductor laser diode by using interferometric photon correlations, i.e., a correlation of photoevents detected at the output ports of an asymmetric Mach-Zehnder interferometer. Earlier methods of interferometric photon correlation measurements were used to study spectral diffusion in organic molecules embedded in solid matrix [28, 29]. The method of interferometric photon correlation we use here was originally applied to differentiate between incoherent light and coherent light with amplitude fluctuations [30]. In contrast to second-order photon correlations, this method

FIG. 1. Experimental setup for measuring interferometric photon correlations. Light from a laser diode enters an asymmetric Mach-Zehnder Interferometer. Single photon avalanche photodetectors (APD) at each output port of the interferometer generate photodetection events, which are time-stamped to extract the correlations numerically.

can clearly distinguish between finite linewidth coherent light and broadband incoherent light [31]. [**XJ: which shows up as separable features in interferometric photon correlation. These separable features have characteristic time constants inversely proportional to the corresponding spectral widths of coherent light and incoherent light. The fraction of coherent light is extracted from the feature associated with coherent light, with a characteristic timescale typically resolvable by the photodetectors used. This eliminates the need for spectral filtering.**] We use this method to extract the fraction of coherent light emitted by the laser diode over a range of pump powers across the lasing threshold.

II. INTERFEROMETRIC PHOTON CORRELATIONS

The setup for an interferometric photon correlation measurement $g^{(2X)}$ is shown in Fig. 1. Light emitted by the laser diode is sent through an asymmetric Mach-Zehnder interferometer, with a propagation delay Δ between the two paths of the interferometer that exceeds the coherence time of the light.

With a light field $E(t)$ at the input, the light fields at the output ports A, B of the interferometer are

$$E_{A,B}(t) = \frac{E(t) \pm E(t+\Delta)}{\sqrt{2}} \,, \qquad (1)$$

with the relative phase shift π acquired by one of the output fields from the beamsplitter.

Using these expressions for the electrical fields, the temporal correlation of photodetection events between the two output ports is given by

$$g^{(2X)}(t_2 - t_1) = \frac{\langle E_A^*(t_1) E_B^*(t_2) E_B(t_2) E_A(t_1) \rangle}{\langle E_A^*(t_1) E_A(t_1) \rangle \langle E_B^*(t_2) E_B(t_2) \rangle} \,. \quad (2)$$

Therein, $\langle \rangle$ indicates an expectation value. and/or an ensemble average. Using Eqn. 1, $g^{(2X)}(t_2 - t_1)$ can be grouped in several terms:

$$
\begin{aligned}
g^{(2X)}&(t_2 - t_1) = \\
&= \frac{1}{4}[\langle E^*(t_1) E^*(t_2) E(t_2) E(t_1) \rangle \\
&\quad + \langle E^*(t_1+\Delta) E^*(t_2+\Delta) E(t_2+\Delta) E(t_1+\Delta) \rangle \\
&\quad + \langle E^*(t_1+\Delta) E^*(t_2) E(t_2) E(t_1+\Delta) \rangle \\
&\quad + \langle E^*(t_1) E^*(t_2+\Delta) E(t_2+\Delta) E(t_1) \rangle \\
&\quad - \langle E^*(t_1+\Delta) E^*(t_2) E(t_2+\Delta) E(t_1) \rangle \\
&\quad - \langle E^*(t_1) E^*(t_2+\Delta) E(t_2) E(t_1+\Delta) \rangle] \,.
\end{aligned}
$$
$$(3)$$

The first two terms have the form of conventional second-order photon correlation functions $g^{(2)}(t_2 - t_1)$. The next two terms are conventional second-order photon correlation functions, time-shifted forward and backward in their argument by the propagation delay Δ. The last two terms reduce $g^{(2X)}$, leading to a dip at zero time difference $t_2 - t_1 = 0$, with a width given by the coherence time of the light.

The expectation values appearing in Eqn. 3 can be evaluated by using statistical expressions [2] of $E(t)$ for incoherent and coherent light [31].

For incoherent light, $g^{(2X)}$ exhibits a "bunching" signature peaking at time differences $\pm\Delta$, $g^{(2X)}(\pm\Delta) = 1 + (1/4)$. At zero time difference, the expected "bunching" signature from conventional second-order photon correlation functions in the first two terms, and the dip from the last two terms of Eqn. 3 cancel each other, resulting in $g^{(2X)}(0) = 1$.

For coherent light, the second-order photon correlation function $g^{(2)} = 1$ combines with the negative contributions from the last two terms of Eqn. 3 such that $g^{(2X)}(0) = 1/2$. [**XJ: As the negative contributions is related to the first-order coherence of the light source, the dip has a shape that is related to the spectral lineshape of the light source by a Fourier transform.**]

III. FRACTION OF COHERENT LIGHT IN A MIXTURE

In order to obtain an interpretation of the nature of the light emitted beyond just presenting the components of $g^{(2X)}$, we consider a light field that is neither completely coherent nor incoherent. We assume that light emitted by the laser is a mixture of coherent light field E_{coh}, and a light field E_{unc} uncorrelated to E_{coh}. The nature of E_{unc}

can be coherent, incoherent, or a coherent-incoherent mixture. [**XJ: As** E_{unc} **may also be light field with a mixture of uncorrelated coherent modes,** E_{coh} **here represents the coherent mode in the mixture of light fields with the brightest intensity.**] In the following, we extract quantitative information about the components of the light field from interferometric photon correlations $g^{(2X)}$, namely the fraction of optical power in the brightest coherent component.

We model the light field mixture with an electrical field

$$E_{\mathrm{mix}}(t) = \sqrt{\rho} E_{\mathrm{coh}}(t) + \sqrt{1-\rho} E_{\mathrm{unc}}(t) , \qquad (4)$$

where ρ is the fraction of optical power the brightest coherent emission, and the respective light field terms are normalised such that $|E_{\mathrm{mix}}| = |E_{\mathrm{coh}}| = |E_{\mathrm{unc}}|$.

Evaluating photon correlation in Eqn. 3 with this light model, and further assuming that first, the propagation delay in the interferometer is significantly longer than the coherence time scale of the light source, and second, the interferometer has good visibility yields

$$g^{(2X)}_{\mathrm{mix}}(0) = 2\rho - \frac{3\rho^2}{2} + \frac{(1-\rho)^2}{2} g^{(2)}_{\mathrm{unc}}(0) \qquad (5)$$

at zero time difference, with only two remaining parameters, ρ and $g^{(2)}_{\mathrm{unc}}(0)$, the second order photon correlation of the uncorrelated field at zero time difference (see Appendix A).

The connection in Eqn. 5, together with the physical requirement $0 \leq \rho \leq 1$ for the fraction of coherent light limits the possible combinations of $g^{(2)}_{\mathrm{unc}}(0)$ and $g^{(2X)}_{\mathrm{mix}}(0)$, shown as non-shaded areas in Fig. 2; the exact expressions for the boundaries are given in Appendix B.

We can now further assume that the uncorrelated light source generates some mixture of coherent and completely incoherent light ($g^{(2)}(0) = 1$), and thermal light ($g^{(2)}(0) = 2$). This constrains the second-order photon correlation of the uncorrelated light:

$$1 \leq g^{(2)}_{\mathrm{unc}}(0) \leq 2. \qquad (6)$$

We impose these bounds in Eqn. 5, and extract the bounds to the fraction of optical power in the brightest coherent emission ρ with an upper bound,

$$\rho \leq \sqrt{2 - 2\, g^{(2X)}(0)}, \qquad (7)$$

and a lower bound,

$$\rho \geq \begin{cases} \frac{1}{2} + \frac{1}{2}\sqrt{3 - 4\, g^{(2X)}(0)}, & \text{for } \frac{1}{2} \leq g^{(2X)}(0) \leq \frac{3}{4} \\ 2 - 2\, g^{(2X)}_{\mathrm{mix}}(0), & \text{for } \frac{3}{4} \leq g^{(2X)}(0) \leq 1 \end{cases}, \qquad (8)$$

with $g^{(2X)}_{\mathrm{mix}}(0)$ ranging from $1/2$ for fully coherent light, to 1 for fully incoherent light.

In practice, these two bounds for ρ are quite tight, and allow to extract the fraction ρ in an experiment with a small uncertainty.

FIG. 2. Combinations of $g^{(2)}_{\mathrm{unc}}(0)$ and $g^{(2X)}_{\mathrm{mix}}(0)$ that correspond to physical and real-valued ρ. In shaded areas, no such solution exist. Inset: Zoom into the region $1 \leq g^{(2)}_{\mathrm{unc}}(0) \leq 2$, where the uncorrelated light source is assumed to be a mixture of coherent and completely incoherent light, and thermal light.

IV. EXPERIMENT

In our experiment, we measure interferometric photon correlations of light emitted from a temperature-stabilised distributed feedback laser diode with a central wavelength around 780 nm.

The setup is shown in Fig. 1. Interferometric photon correlations are obtained from an asymmetric Mach-Zehnder interferometer, formed by 50:50 fibre beamsplitters and a propagation delay Δ of about 900 ns through a 180 m long single mode optical fibre in one of the arms. Photoevents at each output port of the interferometer were detected with actively quenched silicon single photon avalanche photo diodes (APD). The detected photoevents were time-stamped with a resolution of 2 ns for an integration time T.

The correlation function $g^{(2X)}$ is extracted through histogramming all time differences $t_2 - t_1$ between detection event pairs in the inverval T numerically, which allows for a clean normalization.

[**XJ: The dip feature in** $g^{(2X)}$**, is related to the lineshape of the coherent light by a Fourier transform. We assume the coherent light emitted by a laser has a Lorentzian lineshape [32]**] The resulting correlation is fitted to a two-sided exponential function,

$$g^{(2X)}(t_2 - t_1) = 1 - A \cdot \exp\left(-\frac{|t_2 - t_1|}{\tau_c}\right), \qquad (9)$$
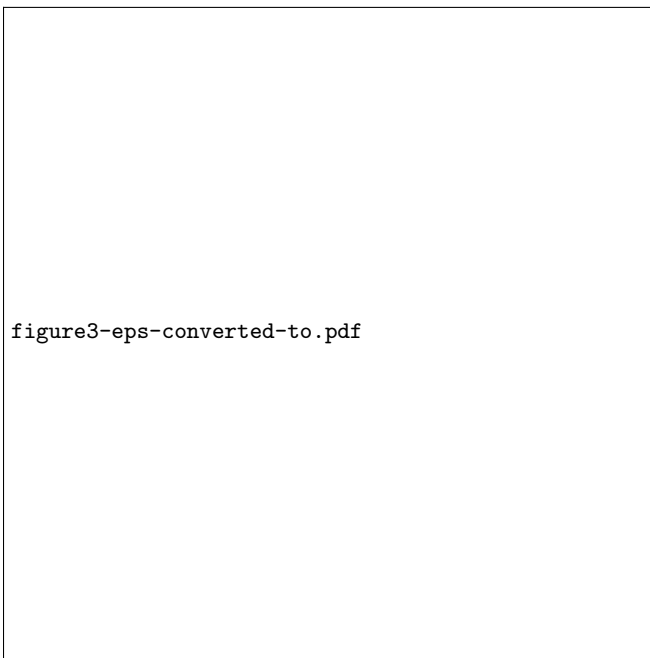
FIG. 3. Interferometric photon correlations $g^{(2X)}$ for different laser currents I_L, extracted from a histogram of photodetector time differences (green symbols). The error range at a specific time bin indicates an expected uncertainty according to a Poissonian counting statistics. The black solid lines show a fit to Eqn. 9, resulting in values for A (from top to bottom) of -0.0006 ± 0.0003, 0.326 ± 0.008, 0.455 ± 0.002, respectively.

where τ_c is the characteristic time constant of the coherent light, and A is the amplitude of the dip. The value of $g^{(2X)}(0)$ is the extracted from the fit as $1 - A$. Examples of measured correlation functions and corresponding fits for different laser powers are shown in Fig. 3.

A. Tranisition from incoherent to coherent light

A transition from incoherent to coherent emission is expected as the laser current is increased across the lasing threshold of the laser. We identify the lasing threshold of a laser diode I_T, by measuring the steepest increase of optical power with the laser current (Fig 4). For our diode, we find $I_T = 37 \, \text{mA}$.

To observe the transition from incoherent to coherent emisssion, we extract the fraction ρ of optical power in the brightest coherent component in the light field at different laser current I_L across the lasing threshold from measurements of $g^{(2X)}$ (Fig. 5, top part). The amplitude of the dip is extracted by fitting these correlations to Eqn. 9, from which the upper bound and lower bound of ρ is extracted (Fig. 5, middle part).

From the fit, ρ remains near 0 below threshold. Above the threshold ρ increases quickly with I_L in a phase-transition manner, reaching $\rho = 0.986$ (90% confidence
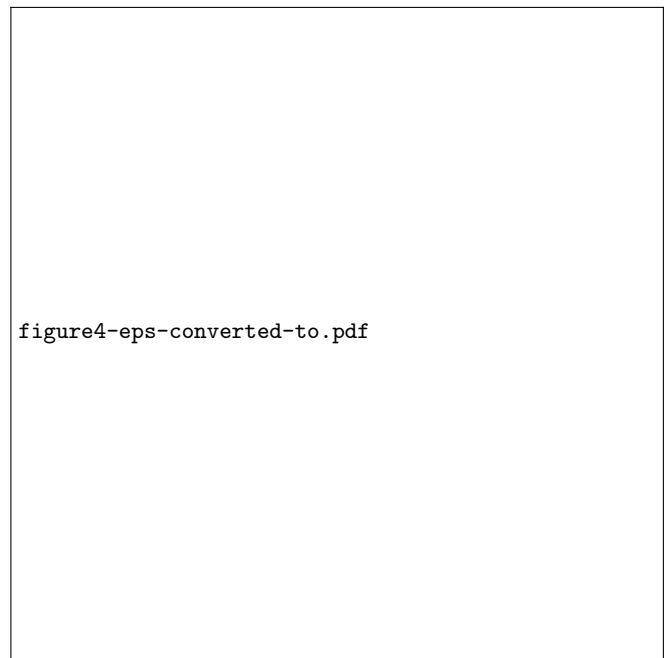

FIG. 4. Measured laser power against laser current I_L. The sharpest change was measured at $I_T = 37 \, \text{mA}$, indicating the threshold current (dashed line).

interval: 0.982 to 0.989) at $I_L = 120 \, \text{mA}$. This agrees with the expectation that the emission of the laser diode is increasingly dominated by stimulated emission when driven with current above the lasing threshold[33, 34].

The upper and lower bounds for ρ from Eqn. 7 and 8 are quite tight even near the lasing threshold, suggesting that the mixture model Eqn. 4 captures the nature of the light through the phase transition well.

The coherence time of the coherent light τ_c can also be extracted from fitting $g^{(2X)}$ measurements to Eqn. 9 (bottom Fig. 5). We observe that the coherence time increases with the current after the threshold current, before reaching a steady value between 300 to 350 ns. The increase of coherence time corresponds to a narrowing of the emission linewidth. This observation agrees with predictions from laser theory that line narrowing is expected with increased pumping [34]. A small modulation of the coherence time becomes visble for larger laser currents, with a periodicity of about 6 mA.

B. Light statistics near a mode hop

Above the threshold, the laser can oscillate at different longitudinal modes for different laser currents. It is interesting to observe the presented method for extracting the fraction of coherent emission near such a mode hop, where two coherent emission modes compete.

For this, the spectrum of light emitted by the laser diode was recorded at different laser currents with an

FIG. 5. Top: Interferometric photon corrrelations $g^{(2X)}$ for different laser currents I_L. Middle: Corresponding upper bound of fraction ρ of coherent light (red) extracted via Eqn. C1, and the lower bound (blue) extracted via Eqn. C2 from $g^{(2X)}(0)$. The dip in ρ is a result of emission at multiple chip modes as explained in Section IV B. The inset shows the extracted bounds for ρ at finer steps of laser current near the lasing threshold. Bottom: Coherence time of coherent light τ_c extracted from $g^{(2X)}$. The dashed line indicates the threshold current $I_T = 37\,\text{mA}$.

FIG. 6. Different chip modes of the laser diode are excited for different currents, resulting in a reduction of the $g^{(2X)}$ signature in a mode competition regime. Top: Power ratios $r_{\alpha,\beta}$ as a function of current for the chip modes α and β around 780.07 nm (solid squares) and 780.34 nm (hollow circles), respectively. Bottom: Upper bound of fraction ρ of coherent light (red) from extracted via Eqn. C1, and the lower bound (blue) extracted via Eqn. C2 from $g^{(2X)}(0)$.

optical spectrum analyser with a spectral resolution of 2 GHz (Bristol 771B-NIR). The laser diode emitted light into two distinct narrow spectral bands with a changing power ratio in the laser current range between 49 mA and 52 mA. Outside this window, only one of the modes could be identified. Below 49 mA, the laser emission was centered around 780.07 nm, above 52 mA around 780.34 nm.

The power fractions $r_{\alpha,\beta}$ of these two chip modes α and β near the mode hop,

$$r_{\alpha,\beta} = \frac{P_{\alpha,\beta}}{P_\alpha + P_\beta}, \tag{10}$$

undergo a nearly linear transition (Fig. 6, top traces).

We measured $g^{(2X)}$ in the same transition regime and extract ρ as described above (Fig. 6, bottom trace). In the transition regime, ρ decreases when both chip modes are present. This can be interpreted as coherent light in one emission band being uncorrelated to coherent light in the other one, but we did not carry out a measurement that would test for a phase relationship between the two modes.

V. CONCLUSION

We presented a method to extract the fraction of coherent light in the emission of a laser by using interferometric photon correlations. As a demonstration, we analyzed light emitted from a diode laser over a range of laser currents, and observe a continuously increasing fraction of coherent light with increasing laser current above the lasing threshold. Applying this technique to light emitted near a mode hop between longitudinal modes suggests a reduction of the fraction of coherent light in the transition regime, and an interpretation that the two longitudinal modes can be viewed as mutually incoherent coherent emissions. Apart from the characterisation of lasers, this method can be useful in practical applications of continuous-variable quantum key distribution protocols, where the noise of lasers as a source of coherent states needs to be carefully characterised to ensure security claims [35–37].

Appendix A: Interferometric photon-correlation for a mixture of light fields

The evaluation of $g^{(2X)}$ via Eqn. 3 requires the conventional second-order photon correlation function $g^{(2)}(t_1 - t_2) = \langle E^*(t_1)E^*(t_2)E(t_2)E(t_1)\rangle$. For the light field mixture Eqn. 4, this is

$$
\begin{aligned}
g_{\mathrm{mix}}^{(2)}(t_2 - t_1) = \\
= \rho^2 \, g_{\mathrm{coh}}^{(2)}(t_2 - t_1) + (1-\rho)^2 \, g_{\mathrm{unc}}^{(2)}(t_2 - t_1) \\
+ 2\rho(1-\rho)\left[1 + \Re[g_{\mathrm{coh}}^{(1)}(t_2 - t_1)\,g_{\mathrm{unc}}^{(1)*}(t_2 - t_1)]\right],
\end{aligned}
\tag{A1}
$$

where $g^{(1)}$ is the first-order field correlation function for the respective component light fields, $g^{(1)*}$ its complex conjugate, and $\Re[\cdots]$ extracts the real part of its argument.

The last term in Eqn. 3 can be written as

$$
\begin{aligned}
\langle E_{\mathrm{mix}}^*(t_1)E_{\mathrm{mix}}^*(t_2+\Delta)E_{\mathrm{mix}}(t_2)E_{\mathrm{mix}}(t_1+\Delta)\rangle \\
= \rho^2\,|g_{\mathrm{coh}}^{(1)}(t_2-t_1)|^2 + (1-\rho)^2|g_{\mathrm{unc}}^{(1)}(t_2-t_1)|^2 \\
+ 2\rho(1-\rho)\,\Re[g_{\mathrm{coh}}^{(1)}(t_2-t_1)\,g_{\mathrm{unc}}^{(1)*}(t_2-t_1)] \\
+ 2\rho(1-\rho)\,\Re[g_{\mathrm{coh}}^{(1)}(\Delta)\,g_{\mathrm{unc}}^{(1)*}(\Delta)],
\end{aligned}
\tag{A2}
$$

where $g^{(1)}(\Delta) \approx 0$ for our experimental situation of the propagation delay Δ being significantly larger than the coherence times of the respective light sources. Note that all terms in Eqn. A2 are real-valued.

With this, the interferometric photon correlation at zero time difference in Eqn. 3 is given by

$$
\begin{aligned}
g_{\mathrm{mix}}^{(2X)}(0) = \\
= \frac{1}{4}[g_{\mathrm{mix}}^{(2)}(\Delta) + g_{\mathrm{mix}}^{(2)}(-\Delta) \\
+ 2(\rho^2\,g_{\mathrm{coh}}^{(2)}(0) + (1-\rho)^2\,g_{\mathrm{unc}}^{(2)}(0) + 2\rho(1-\rho)) \\
- 2(\rho^2\,|g_{\mathrm{coh}}^{(1)}(0)|^2 + (1-\rho)^2|g_{\mathrm{unc}}^{(1)}(0)|^2)].
\end{aligned}
\tag{A3}
$$

We further assume that (1) the propagation delay in the interferometer Δ is significantly longer than the coherence time scale of the light source, such that $g_{\mathrm{mix}}^{(2)}(\pm\Delta) \approx 1$, (2) the interferometer has high visibility such that $|g^{(1)}(0)| \approx 1$, and (3) the second order correlation of the coherent light field is $g_{\mathrm{coh}}^{(2)}(0) = 1$. With this, Eqn. A3 leads to the relationship shown in Eqn. 5.

Appendix B: Boundaries of physically meaningful combinations of interferometric correlations in a mixture

Assuming a binary mixture of the light field as per Eqn. 4, the interferometric correlation of the mixture, $g_{\mathrm{mix}}^{(2X)}(0)$, and the conventional second order correlation of the incoherent light, $g_{\mathrm{unc}}^{(2)}(0)$, at zero time difference are constrained by relation Eqn. 5. Further assuming the physical requirement $0 \le \rho \le 1$ for the fraction ρ gives a lower bound for $g_{\mathrm{unc}}^{(2)}(0)$,

$$
g_{\mathrm{unc}}^{(2)}(0) \ge \begin{cases} 0, & g_{\mathrm{mix}}^{(2X)}(0) \le \frac{2}{3} \\ 3 + \frac{1}{1 - 2g_{\mathrm{mix}}^{(2X)}(0)}, & g_{\mathrm{mix}}^{(2X)}(0) \in [\frac{2}{3}, 1] \\ 2g_{\mathrm{mix}}^{(2X)}(0) & g_{\mathrm{mix}}^{(2X)}(0) \ge 1 \end{cases} .
\tag{B1}
$$

For $g_{\mathrm{mix}}^{(2X)}(0) \in [0, \frac{1}{2})$, there is an upper bound

$$
g_{\mathrm{unc}}^{(2)}(0) \le 2g_{\mathrm{mix}}^{(2X)}(0).
\tag{B2}
$$

Appendix C: Error propagation from fitting of $g^{(2X)}$ measurement

Standard error propagation techniques of experimental data through Eqn. 7-9 lead to infinite uncertainties for some dip amplitudes A and are therefore not used. Instead, we extract upper and lower bounds of ρ. Equation 7 provides an upper bound

$$
\rho \le \sqrt{2A},
\tag{C1}
$$

and Eqn. 8 the lower bound

$$
\rho \ge \begin{cases} 2A, & \text{for } 0 \le A \le \frac{1}{4} \\ \frac{1}{2} + \frac{1}{2}\sqrt{4A-1}, & \text{for } \frac{1}{4} \le A \le \frac{1}{2} \end{cases}
\tag{C2}
$$

for ρ. The probability density for values of A in a measured ensemble is assumed to be a normal distribution, with a mean value and standard deviation extracted from the fit of measured $g^{(2X)}$ to Eqn. 9. This can be transformed into a probability distribution for upper and lower bounds for ρ using Eqns. C1 and C2. We exclude non-physical values of ρ outside $0 \le \rho \le 1$, and renormalize the resulting distribution to compute an expectation value of ρ and a 90% confidence interval shown in Fig. 6.

[1] A. Einstein, Strahlung-emission und-absorption nach der quantentheorie, Verh. d. Deutsche Physik. Ges. **18**, 318 (1916).

[2] R. Loudon, *The Quantum Theory of Light* (Oxford, UK, 2000).

[7] P. Hariharan, *Basics of Interferometry* (Elsevier Academic Press, Amsterdam, Netherlands, 2007).

[8] D. L. Wright, Laser metrology, Developments in Laser Technology I 10.1117/12.946865 (1969).

[9] W. E. Lamb, Theory of an optical maser, Phys. Rev. **134**, A1429 (1964).

[10] F. Arecchi and R. Bonifacio, Theory of optical maser amplifiers, IEEE Journal of Quantum Electronics **1**, 169 (1965).

[11] H. Haken, Cooperative phenomena in systems far from thermal equilibrium and in nonphysical systems, Rev. Mod. Phys. **47**, 67 (1975).

[12] Y.-S. Choi, M. T. Rakher, K. Hennessy, S. Strauf, A. Badolato, P. M. Petroff, D. Bouwmeester, and E. L. Hu, Evolution of the onset of coherence in a family of photonic crystal nanolasers, Applied Physics Letters **91**, 031108 (2007).

[13] S. M. Ulrich, C. Gies, S. Ates, J. Wiersig, S. Reitzenstein, C. Hofmann, A. Löffler, A. Forchel, F. Jahnke, and P. Michler, Photon statistics of semiconductor microcavity lasers, Phys. Rev. Lett. **98**, 043906 (2007).

[14] J. Wiersig, C. Gies, F. Jahnke, M. Aßmann, T. Berstermann, M. Bayer, C. Kistner, S. Reitzenstein, C. Schneider, S. Höfling, A. Forchel, C. Kruse, J. Kalden, and D. Hommel, Direct observation of correlations between individual photon emission events of a microcavity laser, Nature **460**, 245–249 (2009).

[15] R. Hostein, R. Braive, L. L. Gratiet, A. Talneau, G. Beaudoin, I. Robert-Philip, I. Sagnes, and A. Beveratos, Demonstration of coherent emission from high-β photonic crystal nanolasers at room temperature, Opt. Lett. **35**, 1154 (2010).

[16] S. Kreinberg, W. W. Chow, J. Wolters, C. Schneider, C. Gies, F. Jahnke, S. Höfling, M. Kamp, and S. Reitzenstein, Emission from quantum-dot high-ßmicrocavities: Transition from spontaneous emission to lasing and the effects of superradiant emitter coupling, Light: Science & Applications **6**, 10.1038/lsa.2017.30 (2017).

[17] R. Hanbury-Brown and R. Q. Twiss, Correlation between photons in two coherent beams of light, Nature **177**, 27–29 (1956).

[3] R. J. Glauber, The quantum theory of optical coherence, Phys. Rev. **130**, 2529 (1963).

[18] N. Wiener, Generalized harmonic analysis, Acta Mathematica **55**, 117–258 (1930).

[19] A. Khintchine, Korrelationstheorie der stationären stochastischen prozesse, Mathematische Annalen **109**, 604–615 (1934).

[20] L. Mandel and E. Wolf, *Optical Coherence and Quantum Optics* (Cambridge, UK, 1995).

[21] D. B. Scarl, Measurements of photon correlations in partially coherent light, Phys. Rev. **175**, 1661 (1968).

[22] P. K. Tan and C. Kurtsiefer, Temporal intensity interferometry for characterization of very narrow spectral lines, Monthly Notices of the Royal Astronomical Society **469**, 1617 (2017).

[23] R. Centeno Neelen, D. M. Boersma, M. P. van Exter, G. Nienhuis, and J. P. Woerdman, Spectral filtering within the schawlow-townes linewidth of a semiconductor laser, Phys. Rev. Lett. **69**, 593 (1992).

[24] H. P. Weber and H. G. Danielmeyer, Multimode effects in intensity correlation measurements, Phys. Rev. A **2**, 2074 (1970).

[25] J. Yin, S. Zhu, W. Gao, and Y. Wang, Second-order coherence g (2) (τ) and its frequency-dependent characteristics of a two-longitudinal-mode laser, Appl Phys B **64**, 65–72 (1996).

[27] A. George, A. Bruhacs, A. Aadhi, W. E. Hayenga, R. Ostic, E. Whitby, M. Kues, Z. M. Wang, C. Reimer, M. Khajavikhan, and R. Morandotti, Time-resolved second-order coherence characterization of broadband metallic nanolasers, Laser & Photonics Reviews **15**, 2000593 (2021).

[28] X. Brokmann, M. Bawendi, L. Coolen, and J.-P. Hermier, Photon-correlation fourier spectroscopy, Optics Express **14**, 6333 (2006).

[29] L. Coolen, X. Brokmann, and J.-P. Hermier, Modeling coherence measurements on a spectrally diffusing single-photon emitter, Phys. Rev. A **76**, 033824 (2007).

[30] A. Lebreton, I. Abram, R. Braive, I. Sagnes, I. Robert-Philip, and A. Beveratos, Unequivocal differentiation of coherent and chaotic light through interferometric photon correlation measurements, Physical Review Letters **110**, 163603 (2013).

[31] A. Lebreton, I. Abram, R. Braive, I. Sagnes, I. Robert-Philip, and A. Beveratos, Theory of interferometric photon-correlation measurements: Differentiating coherent from chaotic light, Phys. Rev. A **88**, 013801 (2013).

[33] H. Haug and H. Haken, Theory of noise in semiconductor laser emission, Zeitschrift für Physik A Hadrons and nuclei **204**, 262–275 (1967).

[34] H. Haken, *Light: Laser light dynamics* (North-Holland Physics Publishing, Amsterdam, Netherlands, 1981).

[35] Y. Shen, J. Yang, and H. Guo, Security bound of continuous-variable quantum key distribution with noisy coherent states and channel, Journal of Physics B: Atomic, Molecular and Optical Physics **42**, 235506 (2009).

[36] V. C. Usenko and R. Filip, Feasibility of continuous-variable quantum key distribution with noisy coherent states, Phys. Rev. A **81**, 022318 (2010).

[37] Y. Shen, X. Peng, J. Yang, and H. Guo, Continuous-variable quantum key distribution with gaussian source noise, Phys. Rev. A **83**, 052304 (2011).